

ORIGINAL RESEARCH



CD122-targeted interleukin-2 and α PD-L1 treat bladder cancer and melanoma via distinct mechanisms, including CD122-driven natural killer cell maturation

Ryan M Reyes^{a,b,*}, Chenghao Zhang^{b,c,*}, Yilun Deng^b, Niannian Ji^d, Neelam Mukherjee^d, Alvaro S Padron^e, Curtis A Clark^b, Robert S Svatek^{b,d}, and Tyler J Curiel^{b,e}

^aSouth Texas Medical Scientist Training Program, University of Texas Health San Antonio, San Antonio, TX, USA; ^bMays Cancer Center, University of Texas Health San Antonio, San Antonio, TX, USA; ^cXiangya Medical School, Central South University, Changsha, Hunan, China; ^dDepartment of Urology, University of Texas Health San Antonio, San Antonio, TX, USA; ^eDivision of Hematology/Oncology, Department of Medicine, University of Texas Health San Antonio, San Antonio, TX, USA

ABSTRACT

Bladder cancer (BC) and melanoma are amenable to immune checkpoint blockade (ICB) therapy, yet most patients with advanced/metastatic disease do not respond. CD122-targeted interleukin (IL)-2 can improve ICB efficacy, but mechanisms are unclear. We tested α PD-L1 and CD122-directed immunotherapy with IL-2/ α IL-2 complexes (IL-2c) in primary and metastatic bladder and melanoma tumors. IL-2c treatment of orthotopic MB49 and MBT-2 BC generated NK cell antitumor immunity through enhanced activation, reduced exhaustion, and promotion of a mature, effector NK cell phenotype. By comparison, subcutaneous B16-F10 melanoma, which is IL-2c sensitive, requires CD8⁺ T and not NK cells, yet we found α PD-L1 efficacy requires both CD8⁺ T and NK cells. We then explored α PD-L1 and IL-2c mechanisms at distinct metastatic sites and found intraperitoneal B16-F10 metastases were sensitive to α PD-L1 and IL-2c, with IL-2c but not α PD-L1, increasing CD122⁺ mature NK cell function, confirming conserved IL-2c effects in distinct cancer types and anatomic compartments. α PD-L1 failed to control tumor growth and prolong survival in B16-F10 lung metastases, yet IL-2c treated B16-F10 lung metastases effectively even in T cell and adaptive immunity deficient mice, which was abrogated by NK cell depletion in wild-type mice. Flow cytometric analyses of NK cells in B16-F10 lung metastases suggest that IL-2c directly boosts NK cell activation and effector function. Thus, α PD-L1 and IL-2c mediate nonredundant, immune microenvironment-specific treatment mechanisms involving CD8⁺ T and NK cells in primary and metastatic BC and melanoma. Mechanistic differences suggest effective treatment combinations including in other tumors or sites, warranting further studies.

ARTICLE HISTORY

Received 24 July 2021
Revised 9 November 2021
Accepted 9 November 2021

KEYWORDS

Preclinical; immunotherapy; lymphocyte activation; tumor microenvironment; urinary tissue-specific microenvironment; melanoma; bladder cancer; immune checkpoint blockade; IL-2; CD122; NK cells; metastasis



Background

Bladder cancer (BC) and melanoma are among the most common cancers in the United States, collectively accounting for an estimated 190,000 new cancer diagnoses and 25,000 deaths annually.¹ Nearly all cancer-related mortality is from metastases^{2–4} and 5-year survival rates for patients with metastatic BC and melanoma are poor at 6% and 30%, respectively.⁵ BC and melanoma share common metastatic sites, including regional lymph nodes, bones, and lung.^{6,7} Melanoma is also one of the most common extra-abdominal malignancies to develop intraperitoneal metastasis, which is uniformly associated with a poor prognosis.⁸


Immune checkpoint blockade (ICB) antibodies targeting programmed death receptor 1 (PD-1) or one of its ligands (programmed death ligand 1, PD-L1), and cytotoxic T-lymphocyte-associate protein 4 (CTLA-4) have provided durable clinical efficacy in patients with advanced or metastatic melanoma, yet more than 50% do not respond to ICB.^{9–12} BC, like melanoma, is thought to be among the most ICB-responsive cancers due to high tumor mutational burden, yet only 10%–30% of BC patients respond to ICB.¹³

High dose interleukin-2 (IL-2) became a United States Food and Drug Administration-approved metastatic melanoma immunotherapy in 1998, yet is highly toxic with low overall efficacy, in part because of its promotion of regulatory T cells (Tregs).^{14,15} IL-2 signals by binding to the IL-2 receptor (IL-2R), which exists as either a trimer of IL-2R α (CD25), IL-2R β (CD122), and IL-2 R γ (γ c, CD132) subunits or as a dimeric β IL-2 R.^{16,17} Activated T cells and CD4⁺ Foxp3⁺ Tregs express trimeric receptors,¹⁸ whereas memory-phenotype CD8⁺ CD44⁺ T cells and NK cells highly express dimeric β IL-2 R γ and can mediate anti-tumor immunity.¹⁷ Selective dimeric β IL-2R stimulation with CD122-directed IL-2/ α IL-2 complexes (IL-2c) boosts antitumor immunity in murine cancer models by augmenting CD122⁺ effector T cell functions while avoiding the deleterious Treg-promoting effects of IL-2 monotherapy.¹⁹

However, specific effector populations activated by IL-2c are highly dependent on tumor type and the tumor immune microenvironment, which also differentially affects α PD-L1 efficacy despite potentially targeting similar immune populations.²⁰ Here, we studied IL-2c and α PD-L1 immunotherapy treatment mechanisms in orthotopic mouse models

CONTACT Tyler J Curiel  curielt@uthscsa.edu  Department of Medicine, University of Texas Health San Antonio, STRF MC 8252, 8403 Floyd Curl Drive, San Antonio, TX 78229-3900, USA

*Equal contribution and should be considered joint first authors

 Supplemental data for this article can be accessed on the [publisher's website](#)

© 2021 The Author(s). Published with license by Taylor & Francis Group, LLC.

This is an Open Access article distributed under the terms of the Creative Commons Attribution-NonCommercial License (<http://creativecommons.org/licenses/by-nc/4.0/>), which permits unrestricted non-commercial use, distribution, and reproduction in any medium, provided the original work is properly cited.

of BC (MB49 and MBT-2) and melanoma (B16-F10) versus mechanisms in peritoneal and lung metastatic sites. We show that IL-2c promotes NK cell maturation and effector function in distinct primary (orthotopic bladder) and metastatic (peritoneum and lung) sites in a T cell-independent manner. NK cells were indispensable for efficacious treatment of lung metastatic BC and melanoma. Notably, IL-2c effects on CD8⁺ T cells are complementary with α PD-L1 in metastatic melanoma models and treatment effects show tumor and anatomic compartment-dependence. These data shed light on conserved mechanisms of selective IL-2 receptor targeting on NK cell functions and help define treatment response mechanisms, in addition to potentially responsive patient populations, as CD122-directed immunotherapy and ICB combinations are currently in human trials.²¹

Methods

Mice

Wild-type C57BL/6J (BL6) and C3H/HeJ (C3H) mice and B6.129P2-Tcrd^{tm1Mom/J} (TCR δ ^{KO}), B6.129P2-Tcrb^{tm1Mom/J} (TCR β ^{KO}), and B6.129S7-Rag1^{tm1Mom/J} (RAG1^{KO}) genetic knock out mice all on the BL6 background were purchased from The Jackson Laboratory (Bar Harbor, ME). Mice were bred in our animal facility, given *ad libitum* water and food, and housed under specific pathogen-free conditions. All mice were at least 8 weeks old and age- and sex-matched when used for each experiment.

Tumor cell lines and cell culture

Mouse MB49 and MBT-2 BC cell lines were engineered to express luciferase as we described.¹⁹ Mouse B16-F10 (herein B16) was purchased from ATCC (Manassas, VA). We developed Luciferase-expressing B16 using CMV-Firefly luciferase-IRES-Puro lentivirus from Cellomics Technology (Halethrope, MD), following the manufacturer's protocol. All cell lines are PD-L1⁺²²⁻²⁴ and were passaged <5 times prior to tumor challenge. Cells were maintained in 5% fetal bovine serum (FBS)-containing DMEM (Dulbecco's Modified Eagle Medium, MB49, and B16) or RPMI-1640 (Roswell Park Memorial Institute, MBT-2), supplemented with 1/100 dilutions of penicillin/streptomycin, L-glutamate, and 4-(2-hydroxyethyl)-1-piperazineethanesulfonic acid (HEPES).

In vivo tumor challenges

Orthotopic (intravesical) BC challenge with MB49 and MBT-2 used 8×10^4 or 1×10^6 cells, respectively, in 50 μ L Dulbecco's phosphate buffered saline (DPBS, Sigma Aldrich), via indwelling urinary catheter in female mice under isoflurane anesthesia, as described.²⁵ Orthotopic (subcutaneous) B16 challenge used 5×10^5 cells in 200 μ L DPBS into each flank of male mice (2 tumors/mouse). Subcutaneous B16 tumor growth was measured every 2 days by calipers and volume was calculated as (length \times width²)/2. Intraperitoneal B16 challenge used 4×10^5

cells injected into the peritoneum. Lung BC tumors were generated via intravenous tail vein injection of 7×10^5 MB49 or 2.5×10^5 MBT-2 cells in 200 μ L DPBS into male mice.²⁰ Lung B16 tumors were generated via similar methods using 3×10^5 B16 cells. Bladder tumor and peritoneal B16 tumor growth was assessed by tumor weight at sacrifice. Lung B16 tumor growth was measured *in vivo* by tumor bioluminescence every 4 days, starting on day 7 post challenge. Survival was defined as spontaneous death, moribundity, tumor volume ≥ 2000 mm³ (subcutaneous B16), or significant weight loss from baseline ($\geq 15\%$ for bladder and $\geq 20\%$ for lung tumors). To ensure uniform tumor size across all treatment groups, mice were occasionally excluded upon first tumor measurement before randomization, if determined to be an outlier by Grubbs' test.

In vivo bioluminescence monitoring

Bioluminescent imaging (IVIS Lumina Imaging System; Perkin Elmer; Waltham, MA) was used for treatment randomization and *in vivo* tumor monitoring as described.¹⁹ In brief, mice were imaged 15 minutes after intraperitoneal injection of 3 mg PBS-dissolved d-luciferin K⁺ (Gold Biotechnology; St. Louis, MO) with one-minute exposure, small binning, and F/stop = 1. Identical regions of interest were drawn over each mouse and average radiance (photons/sec/cm²/sr) was quantified using Living Image software version 4.2.

In vivo treatments

α PD-L1 (clone 10 F.9G2), α IL-2 (clone JES6-5H4), and isotype control antibodies (clone LTF-2 rat IgG2b and polyclonal Armenian hamster IgG) were purchased from BioXCell (Lebanon, NH). Carrier-free recombinant mouse IL-2 was purchased from Biologend (San Diego, CA). IL-2c is 1.5 μ g/mouse IL-2 complexed with 7.5 μ g/mouse α IL-2 at a 1:2 molar ratio defined as optimal in PBS at 37°C for 15–30 min,²⁶ before intraperitoneal administration in 100 μ L DPBS. IL-2c treatment was every other day for four doses. Treatment began on day 6 or 7 post challenge for orthotopic BC, subcutaneous melanoma, or peritoneal melanoma challenge, and day 7 or 8 for intravenous lung tumor challenge, unless noted otherwise. 100 μ g/mouse α PD-L1 was given intraperitoneally every five days for three doses starting on days 7–9 post tumor challenge, with all experiments using relevant isotype controls.

In vivo cell depletions

α -asialo ganglioside GM1 (asGM1, clone Rabbit) was purchased from FUJIFILM Wako Chemicals U.S.A. Corporation (Richmond, VA) and prepared according to manufacturer's instructions using 1 mL of deionized water. α NK1.1 (clone PK136), α CD8 (clone 2.43), and isotype control antibodies were purchased from BioXCell. Antibodies were given intraperitoneally to deplete relevant cells concurrently with the tumor treatment regimen per figure legends. Doses/mouse: 200 μ L α -asGM1, 250 μ g α NK1.1, and 250 μ g α CD8.

Flow cytometry

Tumors were harvested for flow cytometry after mice were sacrificed via cervical dislocation and induction of deep isoflurane anesthesia. Bladder tumor dissection was as previously described.²⁰ Subcutaneous and peritoneal B16 tumors were dissected and placed in a 6-well plate filled with serum-free RPMI-1640 and manually dissociated with the back of a syringe. Cells were incubated for 45–60 min in 3 mL serum-free RPMI-1640 with 0.25 mg/mL DNase I and 1.65 mg/mL collagenase Type IV (both Sigma Aldrich; St. Louis, MO) and passed through a 70 μ m filter to generate single-cell suspensions. $3\text{--}5 \times 10^6$ cells were then transferred to 96-well plates and samples with $<5 \times 10^6$ cells from the same group were pooled to ensure uniform cell counts for all samples.

Single-cell suspension from lung was prepared as previously reported.²⁷ Briefly, lungs bearing B16 tumors were excised from mice and lung tissue was dissociated via razor blades into fragments of ~1 mm in size. Then, tissue fragments were transferred into a 24-well plate containing 2 mL/lung of digestion medium (complete RPMI containing 2 mg/mL collagenase IV + 0.02 mg/mL DNase I) and incubated at 37°C for 30 min. Cells were then passed through a 70 μ m filter and a single-cell suspension was generated similar to subcutaneous and peritoneal B16 tumors.

Dead cells were excluded using either LIVE/DEAD Fixable Blue Dead Cell Stain Kit for ultraviolet excitation (Thermo Fisher Scientific; Waltham, Massachusetts, USA) or Ghost Dye Violet 510 (Tonbo biosciences; San Diego, California, USA). Fc blocking to prevent nonspecific labeling was done using 1:100 dilution anti-CD16/32 (clone 93, Biolegend). A list of used antibodies, including surface and intracellular staining, is provided in Table 1. Cells were stained for surface antigens by incubating at 4°C for 30–45 min with antibodies against: CD45 (30-F11), CD3 (17A2/145-2C11), CD8 (53–6.7), B220 (RA3-6B2), PD-1 (J43), CD27 (LG.3A10), CD11b (M1/70), CD69 (H1.2F3), CD49b (HMa2), CD122 (TM- β 1), KLRG1 (2F1), NK1.1 (PK136), DNAM-1 (10E5), NKG2A (16a11), and gp100 [EP4863(2)], all at manufacturer recommended dilutions.

For intracellular staining, cells were fixed and permeabilized with FoxP3/transcription factor buffer (eBioscience; San Diego, CA) according to manufacturer instructions, and incubated at 4°C for 45 min. To assess effector molecule production, cells were stimulated with Cell Activator Cocktail (Biolegend) containing phorbol 12-myristate 13-acetate, ionomycin, and brefeldin A at 2 μ L cocktail/mL CR10 medium (RPMI-1640 with 10% FBS, L-glutamine, sodium pyruvate, non-essential amino acids, penicillin/streptomycin, and HEPES buffer) for 6 hours in a 37°C incubator. Following stimulation, intracellular staining was performed by incubating cells at 4°C for 30–45 min with antibodies against: Eomes (W17001A), Perforin (S16009A), Granzyme B (NGZB/GB11), Interferon (IFN)- γ (XMG1.2), all at manufacturer recommended dilutions in FoxP3 permeabilization buffer. Brilliant Stain Buffer Plus (BD) was added to surface and intracellular staining at the manufacturer recommended dilution. Absolute cell numbers were determined by multiplying the cell ratio per live, singlet cell in each flow sample by total cell numbers in the sample.

Table 1. Antibodies and fluorescent dyes used for flow cytometry.

Antibodies	Species	Clone	Fluorochrome	Catalog number	Manufacturer
CD45	Mouse	30-F11	AF532	58–0459-42	eBioscience
	Mouse	30-F11	APC/Fire 810	103174	Biolegend
CD3	Mouse	30-F11	AF700	103128	Biolegend
	Mouse	17A2	BV510	100233	Biolegend
	Mouse	145–2 C11	PE-Cy5	55–0031-U100	Tonbo bioscience
	Mouse	53–6.7	BUV395	563786	BD
CD8a	Mouse	53–6.7	APC-Cy7	25–0081-U025	Tonbo bioscience
	Mouse	53–6.7	APC-Cy7	25–0081-U025	Tonbo bioscience
B220	Mouse	RA3-6B2	BUV661	612972	Biolegend
	Mouse	J43	PerCP-eFlour710	46–9985-82	eBioscience
PD-1	Mouse	J43	BB700	566515	BD
CD27	Mouse/rat/human	LG.3A10	BV605	124249	Biolegend
CD11b	Mouse	M1/70	AF700	101222	Biolegend
	Mouse/human	M1/70	BV570	101233	Biolegend
CD69	Mouse	H1.2F3	PE/Dazzle 594	104535	Biolegend
	Mouse	H1.2F3	BV650	104541	Biolegend
	Mouse	H1.2F3	BUV563	741234	BD
CD49b	Mouse	HMa2	BV711	740704	BD
	Mouse	TM- β 1	BV786	740869	BD
CD122	Mouse	TM- β 1	PE	123210	Biolegend
	Mouse	TM- β 1	PE-Cy5	123219	Biolegend
	Mouse	TM- β 1	PE-Cy5	123219	Biolegend
KLRG1	Mouse	2F1	BV421	566284	BD
	Mouse	PK136	BUV805	741926	BD
NK1.1	Mouse	PK136	BV785	108749	Biolegend
	Mouse	PK136	APC	20–5941-U100	Tonbo bioscience
	Mouse	PK136	APC	20–5941-U100	Tonbo bioscience
CD226 (DNAM-1)	Mouse	10E5	PE/Dazzle 594	128818	Biolegend
NKG2AB6	Mouse	16a11	PerCP-eFlour710	46–5897-82	eBioscience
gp100	Mouse	EP4863(2)	AF647	ab246730	abcam
Eomes	Mouse	W17001A	AF647	157703	Biolegend
	Mouse	S16009A	PE	154306	Biolegend
	Mouse	S16009A	APC	154304	Biolegend
Granzyme B	Mouse/human	GB11	Pacific Blue	515408	Biolegend
	Mouse	NGZB	PE-Cy5.5	35–8898-82	eBioscience
IFN- γ	Mouse	XMG1.2	BUV737	612769	BD

Flow data were acquired on a Cytex Aurora flow cytometer (Cytex Biosciences; Fremont, CA) and analyzed using FlowJo software (BD) version 10.7.1. Representative flow cytometry gating strategies and relevant immune phenotype comparisons across tumor models are shown in *Supplementary Data* and *Table 2*, respectively.

Statistical and data analyses

Data were analyzed and graphed with GraphPad Prism 9.1.2. Data with error bars are mean \pm SEM. To compare two means, we used an unpaired *t* test. Three or more means were compared with one-way ANOVA and *post hoc* Sidak's test. Tumor growth curves were compared by two-way ANOVA, analyzed for overall treatment effect, followed by *post hoc* Sidak's test of discrete time points. Log-rank test was used to compare Kaplan-Meier survival curves. Occasionally, data sets with suspected outliers were identified by Grubbs' test (used only

Table 2. Flow cytometric assessment of NK and CD8⁺ T cell phenotypes across tumor models.

Tumor model	Cell type	Measurement							
		Prevalence	Cell number	Inhibitory receptor	Activation	NK maturation	Function	Additional Markers	
MB49 WT	NK cell	% NK1.1 ⁺ of CD3 ⁻	N/A	PD-1/NKG2A	CD69/DNAM-1	% CD27 ⁻ of NK	% CD69 ⁺ Eomes ⁺ CD27 ⁻ of NK	Perforin	N/A
MBT-2 WT	NK cell	N/A	N/A	N/A	N/A	% CD27 ⁻ NK	% KLRG1 ⁺ of CD27 ⁻ NK	N/A	N/A
MB49 TCRδ ^{KO}	NK cell	% NK1.1 ⁺ of CD3 ⁻	% x Live Cell Count	PD-1	N/A	% and # KLRG1 ⁺ of NK	Eomes ⁺ CD27 ⁻	Perforin	CD11b, CD49b
B16 SQ	CD8 ⁺ T cell	N/A	Normalized to tumor weight	N/A	N/A	N/A	N/A	Perforin	N/A
	NK cell	% NK1.1 ⁺ of CD3 ⁻	N/A	PD-1	N/A	N/A	N/A	Perforin	N/A
B16 IP	CD8 ⁺ T cell	% CD8 ⁺ of CD3 ⁺	N/A	N/A	N/A	N/A	N/A	Perforin/IFN-γ/Granzyme B	CD122
	NK cell	N/A	Normalized to tumor weight	PD-1	CD69	% CD69 ⁺ Eomes ⁺ CD27 ⁻ of NK	N/A	Perforin/Granzyme B	CD122
B16 Lung	CD8 ⁺ T cell	% CD8 ⁺ of CD3 ⁺	Normalized to gp100 ⁺ cell number	N/A	CD69	N/A	N/A	IFN-γ/Granzyme B	N/A
	NK cell	% NK1.1 ⁺ of CD3 ⁻	Normalized to gp100 ⁺ cell number	N/A	CD69	% KLRG1 ⁺ of NK	N/A	IFN-γ/Granzyme B	CD122

WT, wild type. N/A, not applicable. SQ, subcutaneous. IP, intraperitoneal.

once for a given data set) and removed from analysis. For all analyses, significance was based on a multiplicity-corrected α of 0.05.

Results

IL-2c enhances NK cell activation and maturation in orthotopic BC

We previously reported that CD122-targeting IL-2c activated $\gamma\delta$ T cells but not CD8⁺ T cells to treat orthotopic MB49 BC.²⁰ However, effects on other CD122⁺ immune cell populations in bladder are unreported. Like MB49, we observed reduced tumor growth and tumor weight in IL-2c treated mice bearing orthotopic MBT-2 (Fig. S1A,B), a syngeneic mouse BC line on a distinct genetic background (C3H/He) from MB49 (BL6). To assess NK cell effects in IL-2c treatment, we performed flow cytometric analysis of bladders from mice bearing orthotopic MB49 and MBT-2 tumors (Fig. S2). Compared to isotype treatment, IL-2c increased intratumoral NK cell frequency (Figure 1a), reduced PD-1 expression (Figure 1b) and increased CD69 expression (Figure 1c), corresponding with reduced exhaustion and enhanced activation, respectively. We also observed a trend toward decreased expression of the NK cell inhibitory receptor (NKG2A) in IL-2c treated bladders, yet other NK activating receptors (e.g., DNAM-1) were unaffected by IL-2c treatment (Fig. S3A).

NK cell maturation describes the process of terminal differentiation and acquisition of optimal effector function and can be defined by the loss of CD27 expression in nonlymphoid tissues.²⁸ We noted a significant increase in the frequency of CD27⁻ NK cells (Figure 1d) in MB49 tumors, suggesting increased NK cell maturation after IL-2c treatment. Moreover, an increase in frequency of CD69⁺ Eomes⁺ CD27⁻ NK cells (Figure 1e) in the context of efficacious IL-2c treatment suggests that these activated, mature NK cells may be important mediators of the IL-2c driven antitumor immune response. We also observed a trend for increased perforin-producing NK cells after IL-2c treatment

(Fig. S3B), further suggesting IL-2c driven improvement in NK cell effector function. Data in the MBT-2 model corroborated these results, with IL-2c also increasing CD27⁻ NK cell frequency (Fig. S3C) in this model. CD27⁻ NK cells in MBT-2 tumors also highly expressed KLRG1 (Fig. S3D), a marker only present in the final stage of NK cell maturation.²⁹ To test NK contributions to IL-2c efficacy directly, we treated wild-type mice with IL-2c \pm NK cell depletion using α -asialoGM1,³⁰ which significantly reduced treatment efficacy in orthotopic MB49 (figure 1f). Collectively, these data implicate NK cells as critical mediators of IL-2c anti-tumor efficacy in orthotopic bladder tumors through promotion of NK cell maturation and effector function.

IL-2c promotes NK cell maturation in a $\gamma\delta$ T cell-independent manner

We previously reported that antibody-mediated or genetic depletion of $\gamma\delta$ T cells significantly abrogated IL-2c efficacy in orthotopic MB49 challenge,²⁰ similar to NK cell depletion shown here (figure 1f). Thus, we hypothesized that IL-2c treatment efficacy is either the summation of independent $\gamma\delta$ T and NK cell effects or the result of their coordinated interactions. To test interactions, we performed flow cytometric analysis of intratumoral bladder NK cell content in orthotopic MB49 challenged TCRδ^{KO} mice (lacking all $\gamma\delta$ T cells) \pm IL-2c treatment. As in wild-type mice (Figure 1), IL-2c NK cell effects included increased intratumoral bladder NK cell frequency (Figure 2a), reduced PD-1 expression (Figure 2b), and increased frequency of perforin-producing NK cells (Figure 2c). We then evaluated if the NK cell maturation phenotype observed in IL-2c treated wild-type mice was also present in TCRδ^{KO} mice. As in wild-type mice, we found a robust increase in the frequency and number of NK cells co-expressing KLRG1 and Eomes (Figure 2d,e), both of which are essential for NK cell maturation and function.^{29,31} These data suggest that IL-2c driven NK cell maturation in this model appears to be $\gamma\delta$ T cell independent, suggesting potential benefits of IL-2c in other contexts.

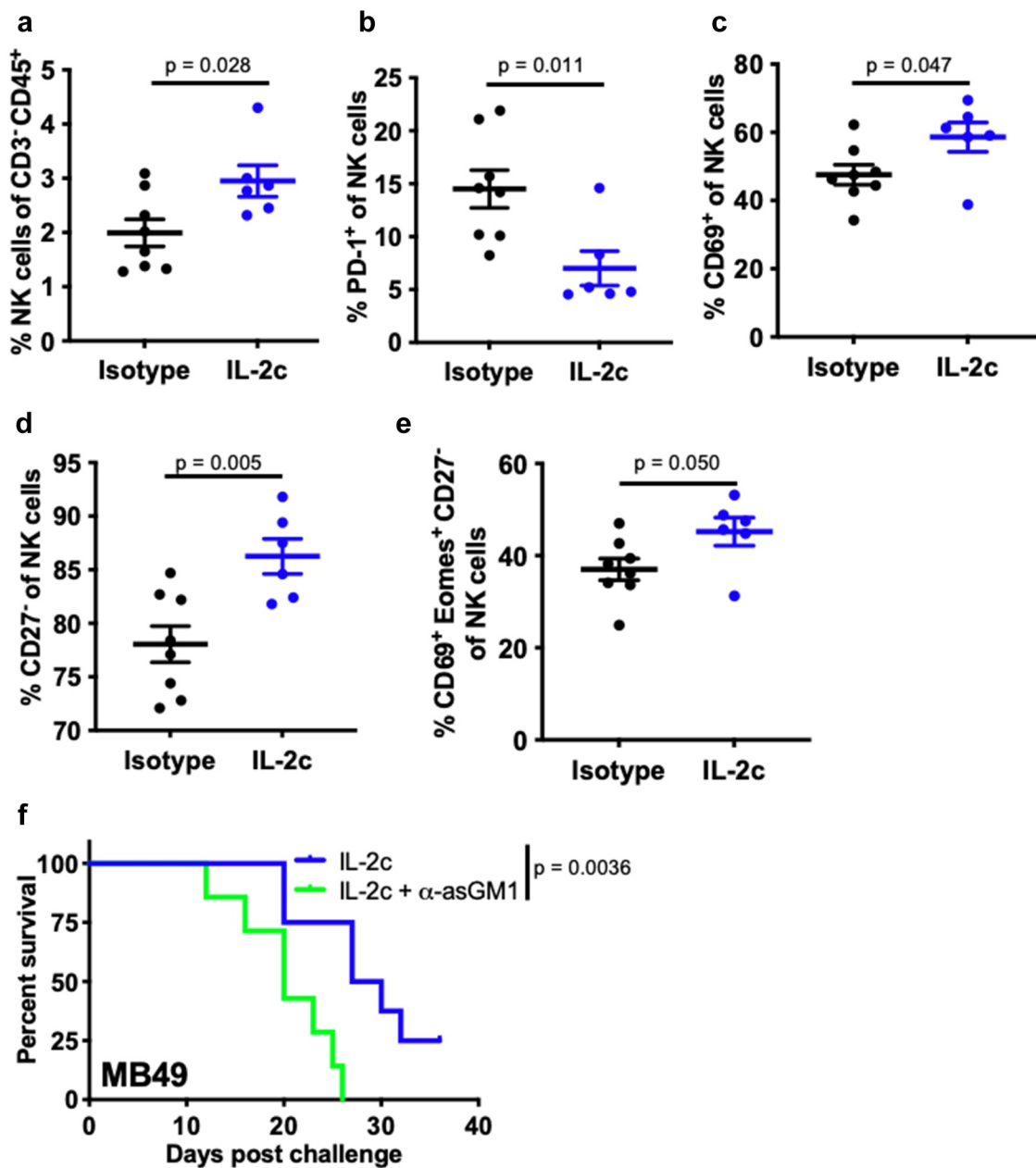


Figure 1. IL-2c enhances NK activation and maturation to treat orthotopic BC. Wild-type female mice were challenged orthotopically with 8×10^4 MB49 and treated with IL-2c or an isotype control every other day starting on day 7 for a total of 4 doses. (a-e) Mice were sacrificed on day 16 post challenge. Flow cytometric analysis of intratumoral bladder NK cell frequency (a), exhaustion (PD-1⁺) (b), activation (CD69⁺) (c), maturation (CD27⁻) (d), and CD69⁺ Eomes⁺ expression by CD27⁻ NK cells (e). N = 6–8 pooled bladders/group. p, unpaired t test. NK cells in MB49 defined as CD45⁺ CD3⁺ NK1.1⁺ cells. (f) Mouse survival in orthotopic MB49 challenge treated with IL-2c (as above) \pm 200 μ L α -asialo GM1 (α sGM1). N = 7–9 mice/group. p, log-rank. Note: We previously reported data showing survival of isotype-treated mice bearing orthotopic MB49.²⁰ Eomes, Eomesodermin. IL-2c, interleukin-2 complex. NK, Natural Killer. PD-1, Programmed Death Receptor 1.

We then performed more detailed analyses of NK cell maturation in TCR δ^{KO} mice bearing orthotopic MB49 by examining CD49b⁺ NK cells, as CD49b is a marker acquired at the onset of NK cell maturation in BL6 mice.²⁹ Using differential expression of CD11b and CD27 to evaluate the final three stages of NK cell maturation,³² we found that IL-2c significantly increased the frequency of terminally differentiated, mature CD11b⁺ CD27⁻ NK cells (Fig. S4A,B), with striking increases in KLRG1⁺ NK cell frequency (Fig. S4C), as observed in wild-type hosts (Figure 1). IL-2c also increased the number of Perforin⁺ Eomes⁺ KLRG1⁺ mature NK cells (Fig. S4D) suggesting enhanced effector function.

aPD-L1 requires CD8⁺ T and NK cells to treat subcutaneous B16 melanoma

IL-2 activates downstream STAT5 signaling via CD122 in NK cells and facilitates NK cell cytotoxicity,³³ yet prior studies in subcutaneous B16 melanoma showed that CD8⁺ T cells but not NK cells, are required for IL-2c treatment efficacy.³⁴ To determine if lack of NK cell requirements for IL-2c treatment efficacy in orthotopic B16 is tissue microenvironment-specific, we studied α PD-L1 which has established effects on CD8⁺ T and NK cells in several cancers.³⁵ We confirmed α PD-L1 efficacy in B16 in our mice (Figure 3a), consistent with prior

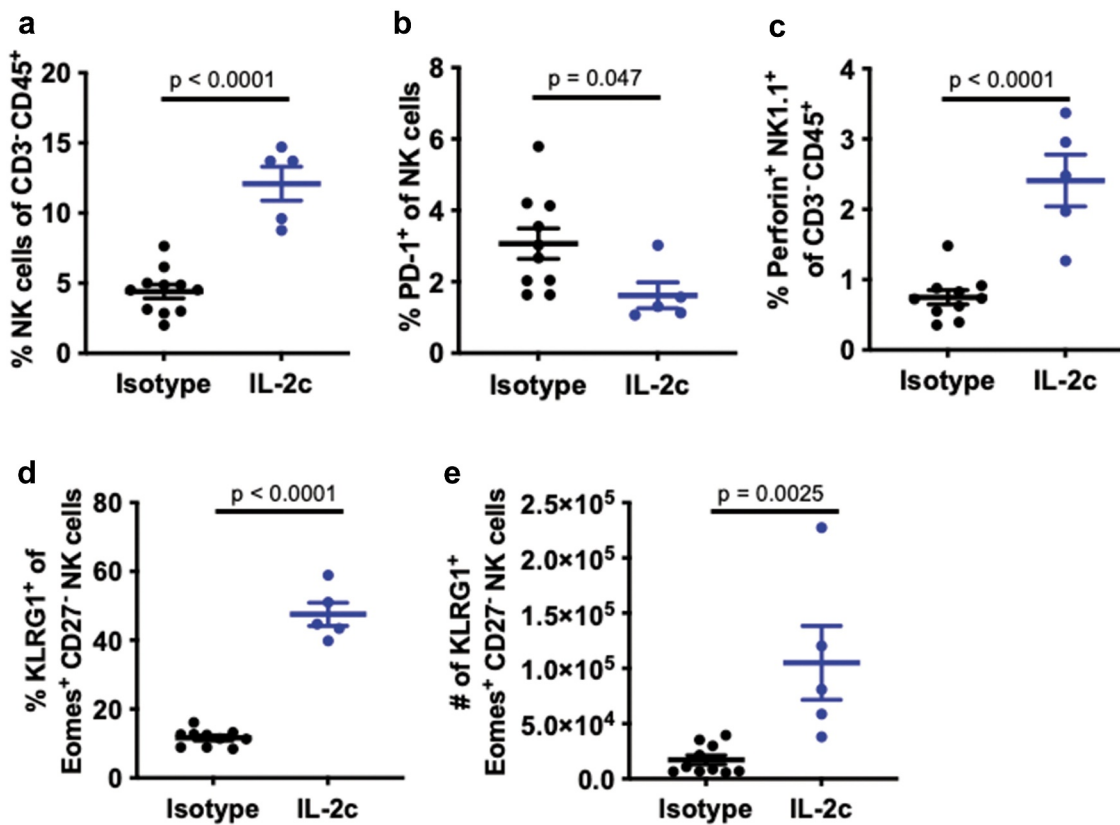


Figure 2. IL-2c promotes NK cell maturation in a $\gamma\delta$ T cell independent manner. TCR5^{KO} female mice were challenged orthotopically with 8×10^4 MB49 cells and treated with IL-2c on days 9, 11, 13, and 15 or isotype control. Mice were sacrificed on day 17 for flow cytometric analysis of NK cell frequency (a), exhaustion (i.e., PD-1⁺) (b), perforin production (c), and KLRG1⁺ Eomes⁺ expression by CD27⁻ NK cells (d,e). NK cells in MB49 defined as CD45⁺ CD3⁺ NK1.1⁺ cells. N = 9–11 mice/group. Tumors were pooled to achieve 5×10^6 live cells per sample. p, unpaired t test. Eomes, Eomesodermin. IL-2c, interleukin-2 complex. KLRG1, Killer Cell Lectin Like Receptor G1. NK, Natural Killer. PD-1, Programmed Death Receptor 1.

reports.^{36,37} Flow cytometric analysis of subcutaneous B16 tumors (Fig. S5) showed that α PD-L1 improved CD8⁺ T cell number (Figure 3b) and effector function detected as increased perforin expression (Figure 3c), consistent with enhanced T cell cytotoxicity. However, α PD-L1 also increased intratumoral NK cell frequency (Figure 3d), reduced PD-1 expression (Figure 3e), and increased prevalence of perforin-producing NK cells (figure 3f), showing the potential for beneficial α PD-L1 effects on NK cells in skin. We then depleted CD8⁺ T cells with α CD8 (Fig. S6) or NK cells with α -asialoGM1 during α PD-L1 treatment and found that both depletions significantly abrogated α PD-L1 mediated tumor control of subcutaneous B16 melanoma (Figure 3g). Together, these data confirm distinct tumor microenvironment-dependent effects of IL-2c and α PD-L1 in treatment of orthotopic (primary) B16 and provide an important baseline for comparison with mechanisms of these agents at metastatic sites.

IL-2c or α PD-L1 alone treat peritoneal B16 melanoma

We have extensively studied orthotopic (peritoneal) ID8agg mouse ovarian cancer, which is refractory to α PD-L1 but sensitive to IL-2c.¹⁹ To compare IL-2c and α PD-L1 mechanisms in orthotopic (subcutaneous) B16 and ID8agg, we used a clinically relevant peritoneal metastatic melanoma model⁸ via intraperitoneal injection of B16 into wild-type mice.³⁸ Peritoneal tumors from α PD-L1 treated mice were marginally

smaller than isotype controls, yet IL-2c treatment led to a dramatic reduction in tumor weight versus isotype and α PD-L1 treated mice (Fig. S7A). Both agents equally improved mouse survival (Fig. S7B).

IL-2c promotes NK cell maturation in peritoneal B16, whereas α PD-L1 does not

Flow cytometric analyses of peritoneal B16 tumors (Fig. S8) showed that IL-2c increased total intratumoral CD45⁺ immune cell content (Figure 4a) compared to isotype control and α PD-L1 treated mice. α PD-L1 and IL-2c shared many beneficial effects on CD8⁺ T cells including increasing their prevalence (Figure 4b) and production of effector molecules including perforin, IFN- γ , and granzyme B (Figure 4c-e), yet IL-2c effects were superior to α PD-L1 in these regards (Figure 4b-e). IL-2c also had NK cell activating effects not elicited by α PD-L1, including increased NK cell concentration (Fig. S9A) and CD69 expression (Fig. S9B), though both agents reduced NK cell PD-1 expression versus isotype controls (Fig. S9C). IL-2c-mediated NK activation also increased effector molecule production (figure 4f,g), frequency of CD69⁺ Eomes⁺ CD27⁻ activated mature NK cells (Figure 4h), and increased NK cell CD122 expression (Figure 4i), effects not observed with α PD-L1 (figure 4f-i).

To assess CD8⁺ T and NK cell contributions to α PD-L1 and IL-2c treatment mechanisms, we administered α PD-L1 \pm CD8⁺ T and NK cell depleting antibodies to peritoneal B16 tumor-bearing

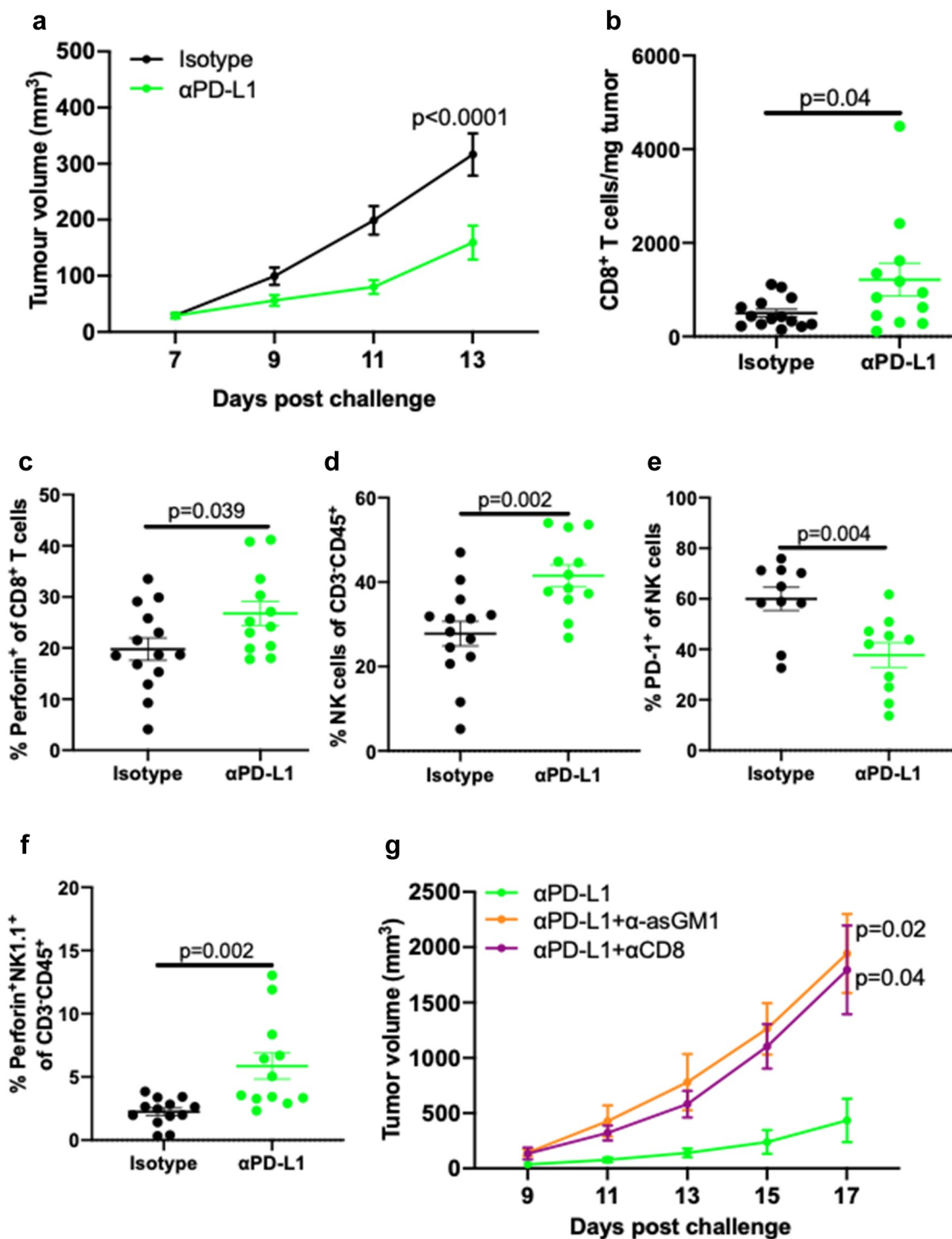


Figure 3. αPD-L1 requires NK and CD8⁺ T cells to treat subcutaneous B16 melanoma. Wild-type male mice were challenged subcutaneously with 5×10^5 B16 cells on both flanks and treated with 100 μg αPD-L1 on days 7, 12, 17 or an isotype control (a-f). (a) Tumor growth of mice bearing subcutaneous B16. N = 7 mice/group. p, two-way ANOVA of day 13 tumor volume. (b-e) Mice were sacrificed on day 14 for flow cytometric analysis of CD8⁺ T cell number (b) and perforin production (c), and NK cell prevalence (d), exhaustion (i.e., PD-1⁺) (e), and perforin production (f). N = 6–7 mice/group. p, unpaired t test. (g) Wild-type male mice were challenged subcutaneously with 5×10^5 B16 cells on a single flank and treated with 100 μg αPD-L1 on days 7, 10, and 13 ± 200 μL α-asGM1, 250 μg αCD8, or an isotype control every three days starting the day before the challenge until the end of αPD-L1 treatment. N = 5 mice/group. p, two-way ANOVA of day 17 tumor volume. ANOVA, analysis of variance. asGM1, asialo GM1. NK, Natural Killer. PD-L1, Programmed Death Ligand 1. PD-1, Programmed Death Receptor 1.

mice. Consistent with our flow cytometric analyses that showed αPD-L1 effects primarily via CD8⁺ T cells and not NK cells in this model, CD8⁺ T cell depletion significantly reduced survival of mice treated with αPD-L1, whereas NK cell depletion did not impact survival (Figure 4j). As CD8⁺ T cell depletion did not

fully abrogate treatment efficacy, other immune cells likely also contribute. IL-2c treatment of peritoneal B16 had similar CD8⁺ T cell requirements, yet surprisingly, NK cell depletion did not significantly reduce survival (Figure 4k). This may be due to the strength of IL-2c CD8⁺ T cell effects in this context compared to

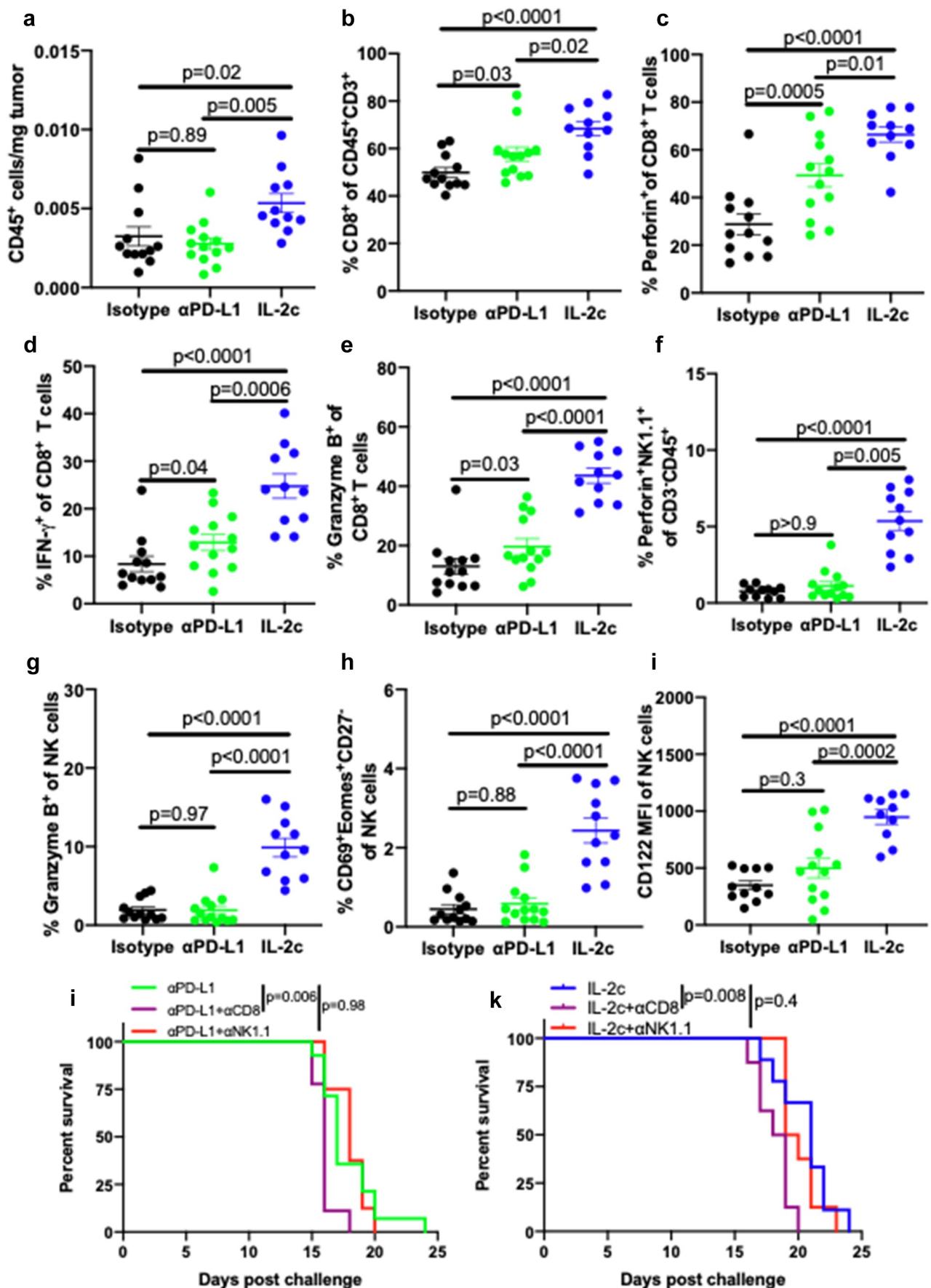


Figure 4. IL-2c activates CD8⁺ T cells and promotes NK cell maturation in peritoneal B16. Wild-type male mice were challenged peritoneally with 4×10^5 B16 cells and treated with 100 μg αPD-L1 on days 7, 12, 17 or IL-2c on days 7, 9, 11, 13. Mice were sacrificed on day 15 for flow cytometric analysis of immune (CD45⁺) cell number normalized to tumor weight (a). (b-e) Intratumoral CD8⁺ T cell frequency (b) and effector molecule production (c-e). (f-i) Intratumoral NK cell perforin (f) and granzyme B

(g) production, CD69⁺ Eomes⁺ expression by CD27⁻ NK cells (h), and CD122 expression (i). N = 11–13 mice/group. *p* value, one-way ANOVA. (j) Survival of wild-type male mice challenged peritoneally with 4×10^5 B16 cells and treated with α PD-L1 (as above) \pm 250 μ g α NK1.1 or 250 μ g α CD8 on days 6, 9, 12, 15, 18. N = 8–14 mice/group. *p* value, log-rank. (k) Survival of wild-type male mice challenged peritoneally with 4×10^5 B16 cells and treated with IL-2c (as above) \pm 250 μ g α NK1.1 or 250 μ g α CD8 on days 6, 9, 12, 15. N = 8–9 mice/group. *p* value, log-rank. Note: Survival of mice in Figure 4j,k can be compared to survival of isotype-treated mice with peritoneal B16 in Fig. S7B. ANOVA, analysis of variance. Eomes, Eomesodermin. IFN- γ , interferon-gamma. IL-2, interleukin-2 complex. MFI, Mean Fluorescence Intensity. NK, Natural Killer. PD-L1, Programmed Death Ligand 1.

NK cells, as CD8⁺ T cells expressed higher levels of CD122 (the IL-2c target) both at baseline and during IL-2c treatment (Fig. S9D). These data show that in addition to many shared effects on CD8⁺ T cells with α PD-L1, IL-2c-mediated promotion of NK cell maturation and function extends across tumor types and anatomic locations, though specific contributions of pleiotropic IL-2c immune effects to immunotherapy efficacy is tumor microenvironment-specific.

IL-2c treats B16 lung metastases, whereas α PD-L1 is ineffective

The lung is the most common site of visceral metastasis in melanoma³⁹ and approximately one-third of BC metastases are to the lungs.^{7,40} We previously showed that IL-2c and α PD-L1 fail as single-agent treatments in lung metastatic MB49 or MBT-2 BC, but their combination was effective and required CD8⁺ T cells.²⁰ To test if treatment mechanisms were cancer-

specific, we studied a model of melanoma lung metastasis via intravenous B16 cell injection. As in BC lung metastasis, α PD-L1 was unable to slow tumor growth (Figure 5a) or prolong mouse survival (Figure 5b) in lung metastatic B16 melanoma despite its efficacy in subcutaneous (Figure 3) and peritoneal (Fig. S7) metastases. However, IL-2c significantly slowed B16 lung metastatic tumor growth (Figure 5c) and improved survival as a single agent versus isotype treated controls (Figure 5d), mirroring outcomes in orthotopic (peritoneal) ID8agg ovarian cancer which is also IL-2c sensitive but α PD-L1 resistant.¹⁹

IL-2c treatment efficacy in lung metastasis is NK cell-dependent

Next, we tested if treatment mechanisms for IL-2c treatment efficacy in B16 lung metastases were similar to subcutaneous or peritoneal B16. Using TCR β ^{KO} mice that lack CD4⁺ and CD8⁺ T cells, we found that IL-2c still reduced B16 lung tumor growth

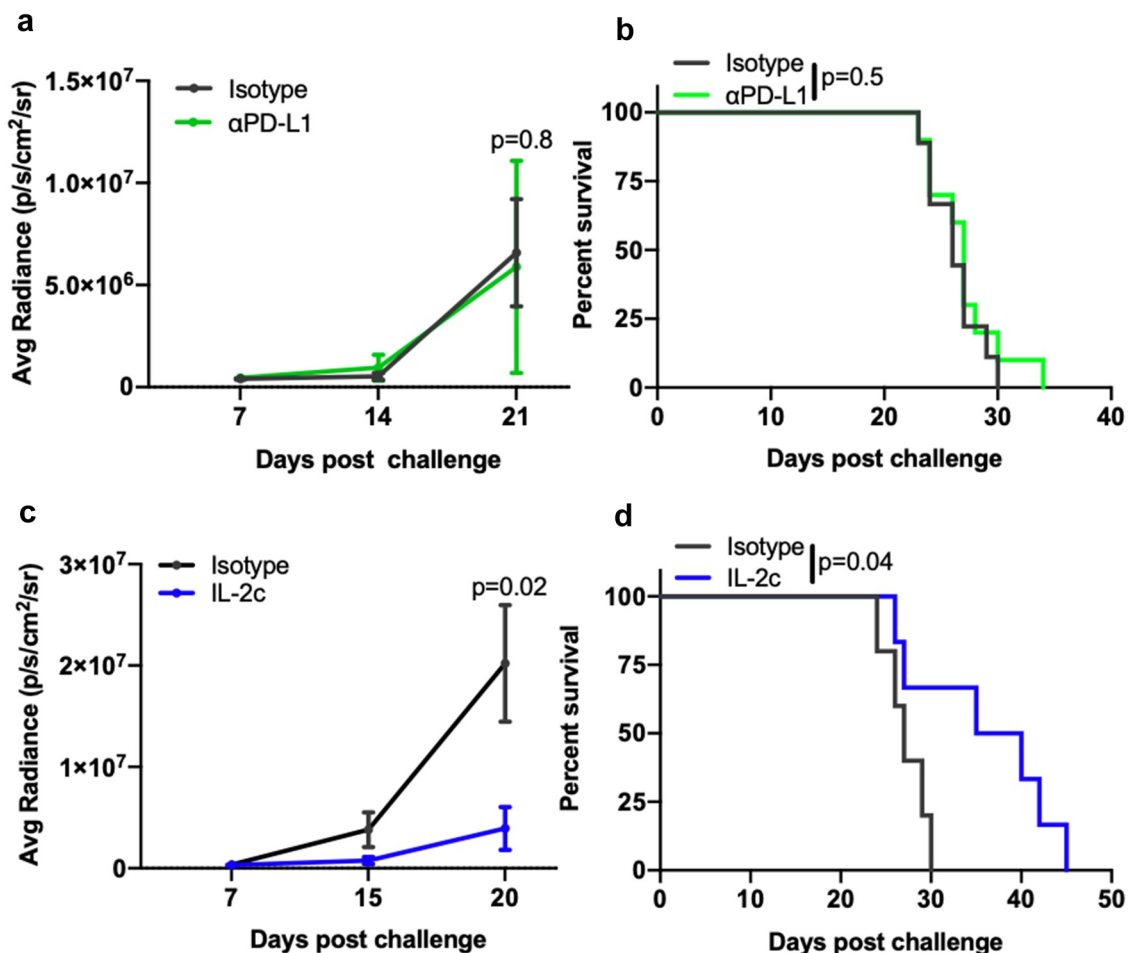


Figure 5. IL-2c, but not α PD-L1, treats B16 lung metastases. Wild-type male mice were challenged intravenously with 3×10^5 B16 cells and treated with 100 μ g α PD-L1 (a, b) on days 8, 13, 18, or IL-2c (c, d) on days 8, 10, 12, 14, or isotype control (a-c). (a, c) Tumor bioluminescence corresponding with pre-treatment, mid-treatment, and post treatment timepoints. N = 6–10 mice/group. *p*, two-way ANOVA of day 21 (a) or 20 (c) signal. (b, d) Mouse survival of mice in (a) and (c). N = 6–10 mice/group. *p*, log-rank. ANOVA, analysis of variance. IL-2c, interleukin-2 complex. PD-L1, Programmed Death Ligand 1.

(Figure 6a) and improved mouse survival versus isotype control treatment (Figure 6b). IL-2c acts through $\gamma\delta$ T cells in orthotopic bladder cancer (Figure 6b). IL-2c acts through $\gamma\delta$ T cells in orthotopic bladder cancer (Figure 6b). To assess possible $\gamma\delta$ T cell effects in B16 lung metastases, we challenged RAG1^{KO} mice, which additionally lack $\gamma\delta$ T cells and B cells compared to TCR β ^{KO} mice. IL-2c still improved mouse survival versus controls (Figure 6c), supporting the concept that IL-2c treats lung metastatic B16 independent of adaptive immunity or $\gamma\delta$ T cells.

As IL-2c significantly promoted NK cell activity in both orthotopic BC (Figure 1) and metastatic melanoma models (Figure 4), we tested NK cell-driven antitumor immunity as a mediator of IL-2c efficacy in metastatic B16 lung tumors. We depleted NK cells using α NK1.1 (Fig. S10) in mice bearing lung metastatic B16 melanoma treated with IL-2c, which reduced IL-2c-mediated control of tumor growth (Figure 6d) and survival (Figure 6e), supporting a critical role for NK cells in IL-2c efficacy here.

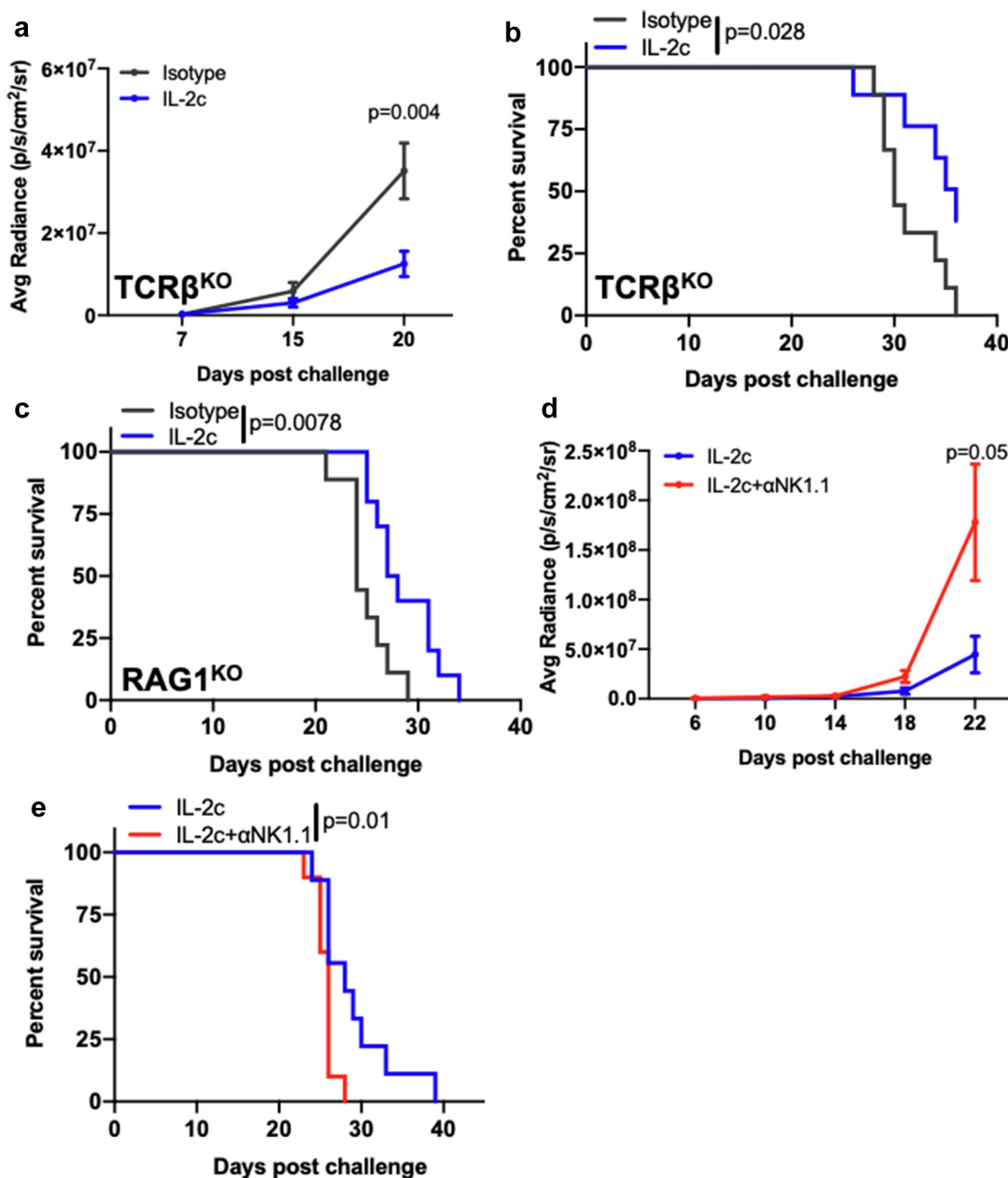


Figure 6. NK cells are essential for IL-2c efficacy in lung metastasis. TCR β ^{KO} (a, b), RAG1^{KO} (c), or wild-type (d, e) male mice were challenged intravenously with 3×10^5 B16. (a-e) Mice received IL-2c on days 8, 10, 12, 14, an isotype control (a-c), or 250 μ g α NK1.1 on days 7, 10, 13, 16 (d, e). (a) Tumor bioluminescence in intravenous B16 challenge of TCR β ^{KO} mice. N = 9–10 mice/group. p, two-way ANOVA of day 20 signal. (b) TCR β ^{KO} mouse survival following intravenous B16 challenge. N = 9–10 mice/group. p, log-rank. (c) RAG1^{KO} mouse survival following intravenous B16 challenge. N = 9 mice/group. p, log-rank. (d) Tumor bioluminescence in intravenous B16 challenge of wild-type mice. N = 11–12 mice/group. p, two-way ANOVA of day 22 signal. (e) Wild-type mice survival following intravenous B16 challenge. Note: Survival of isotype-treated mice bearing B16 lung metastasis is in Figure 5d. N = 11–12 mice/group. p, log-rank. ANOVA, analysis of variance. RAG1, Recombinase Activating Gene 1. TCR, T Cell Receptor.

In lung metastatic MB49 and MBT-2 BC, IL-2c, or α PD-L1 alone are ineffective, but their combination effectively treats both models.²⁰ To test NK cell contributions to treatment of lung metastases in BC, we challenged mice with either lung metastatic MB49 or MBT-2 and treated with α PD-L1 + IL-2c with or without NK cell depletion (Fig. S11). In support of significant NK cell contributions, NK cell depletion significantly reduced mouse survival in both models (Fig. S12A,B). Together, these data show that IL-2c effects on NK cells are disparate from CD8⁺ T cell effects and contribute independently to immunotherapy efficacy across multiple primary (orthotopic) and metastatic models of BC and melanoma on distinct genetic backgrounds.

IL-2c activates lung NK cells to treat B16 lung metastases

We then performed flow cytometric analyses of B16 lung tumors (Fig. S13) to explore possible mechanisms for NK cell-mediated IL-2c efficacy in lung. We used gp100⁺ (melanoma-associated antigen⁴¹) cell number to normalize tumor-infiltrating NK and CD8⁺ T cell numbers and found that IL-2c but not α PD-L1, significantly increased the frequency (Figure 7a) and total numbers (Figure 7b) of lung tumor-infiltrating NK cells, as well as numbers of activated NK cells (Figure 7c). IL-2c also improved NK cell production of anti-tumor effector molecules granzyme B and IFN- γ (Figure 7d,e), and increased CD122 expression (figure 7f), with α PD-L1 having no observable NK cell effects (Figure 7a-f). Similar to orthotopic MB49 BC, IL-2c treatment also significantly increased expression of the NK cell maturation marker KLRG1 (Figure 7g), consistent with terminal differentiation and enhanced effector function of lung NK cells.

In contrast, neither IL-2c nor α PD-L1 treatment affected CD8⁺ T cell prevalence (Fig. S14A), total numbers (Fig. S14B), activation (Fig. S14 C), or effector molecule production (Fig. S14D). These results support our findings in T cell deficient mice (Figure 6a-c) that CD8⁺ T cells are dispensable for IL-2c efficacy in B16 lung metastasis and further emphasize the role of NK cells in mediating the IL-2c efficacy in this model.

Discussion

ICB with α PD-1 or α PD-L1 is FDA-approved to treat nearly 20 cancer subtypes⁴² yet even in the most ICB-sensitive cancers, many patients do not respond,⁴³ necessitating improved treatment approaches. Here, we studied IL-2c and α PD-L1 treatment mechanism differences in primary (orthotopic) and metastatic BC and melanoma, heading toward our goal of identifying conserved immune cell intrinsic mechanisms of these two agents that persist in varied tumor immune microenvironments, which could help define rational treatment combinations for improved treatment efficacy.

We previously reported that $\gamma\delta$ T cells were required for optimal IL-2c treatment efficacy in orthotopic bladder cancer²⁰ and recently showed that $\gamma\delta$ T cells augment antigen-specific immunity in the treatment of MB49 BC with Bacillus Calmette-Guérin (BCG) immune therapy.⁴⁴ Here, we found that NK cells also contribute to IL-2c efficacy in orthotopic bladder cancer in a $\gamma\delta$ T cell-independent manner, suggesting that both cells could contribute individually, rather than

serially, to treatment efficacy. Thus, strategies to boost function of either cell type could improve IL-2c efficacy, such as ultra-low dose rapamycin, which we demonstrated to be a safe and tolerable $\gamma\delta$ T cell adjuvant in early phase BC trials when combined with BCG immune therapy.⁴⁵

To understand tissue-selective effects and assess differences from α PD-L1, we found that α PD-L1 required both CD8⁺ T cells and NK cells to treat orthotopic B16 melanoma, whereas IL-2c only required CD8⁺ T cells.³⁴ These data show that IL-2c has differential mechanisms of action against the same tumor in distinct anatomic compartments, and that α PD-L1 effects in the same environment and tumor can differ from IL-2c. Our prior study showed that CD8⁺ T cells are dispensable for IL-2c treatment of orthotopic bladder cancer (where $\gamma\delta$ T cells²⁰ and NK cells (this report) are required), whereas α PD-L1 requires CD8⁺ T cells to treat orthotopic bladder cancer, suggesting potential benefit of combining both agents. We also found that NK cells from IL-2c treated mice consistently expressed lower PD-1, which could also impact ICB therapy. Further studies evaluating the impact of CD122-directed IL-2 therapy on ICB targets (e.g., PD-1, PD-L1) are warranted to gain better mechanistic insights that can facilitate optimized combination therapies.

We considered that metastatic tumors represent an additional immune challenge to hosts, whereby the tumor appears in distinct anatomic compartments. To understand IL-2c and α PD-L1 effects in metastatic tumors, we evaluated peritoneal B16 melanoma, a large unmet clinical need, as patients with peritoneal metastatic melanoma have a median survival of only two months.⁸ We found that either IL-2c or α PD-L1 alone effectively treated, but did not cure, peritoneal B16. By contrast, we previously showed that IL-2c very effectively treated peritoneal (orthotopic) ID8agg ovarian cancer, where α PD-L1 is entirely ineffective.¹⁹ Thus, these outcomes do not reflect the generic efficacy of α PD-L1 in the peritoneal compartment. In peritoneal B16, IL-2c activated CD8⁺ T cells more effectively versus NK cells, which could be due to greater CD122 expression on local CD8⁺ T cells versus NK cells that we show here. Cell depletion data were consistent with flow data for α PD-L1 efficacy mechanisms, but not for IL-2c. IL-2c greatly improved NK cell numbers and functions over α PD-L1, yet NK cell depletion very surprisingly did not affect IL-2c treatment efficacy in peritoneal B16. There are several potential explanations that require further investigations. Among these, the NK cell effects required for treatment efficacy might not be reflected in flow analyses, specific suppressive factors could impede NK cell efficacy after IL-2c but not after α PD-L1, and NK cell/tumor co-localization could differ based on IL-2c versus α PD-L1 treatments. These data underscore the fact that flow cytometric analyses in this model might not fully reflect all mechanistic details. Further, as CD8⁺ T cell depletion did not fully reverse IL-2c treatment efficacy in peritoneal metastases, additional mechanisms might exist, requiring further studies.

In the clinically relevant setting of B16 melanoma lung metastases, IL-2c outperformed α PD-L1 in tumor control and host survival. As α PD-L1 treats subcutaneous B16, these data show that the local immune microenvironment can significantly affect treatment efficacy. In accord with much other data here, IL-2c efficacy in lung metastases depended on NK cells. Further, lung metastatic IL-2c efficacy was independent of

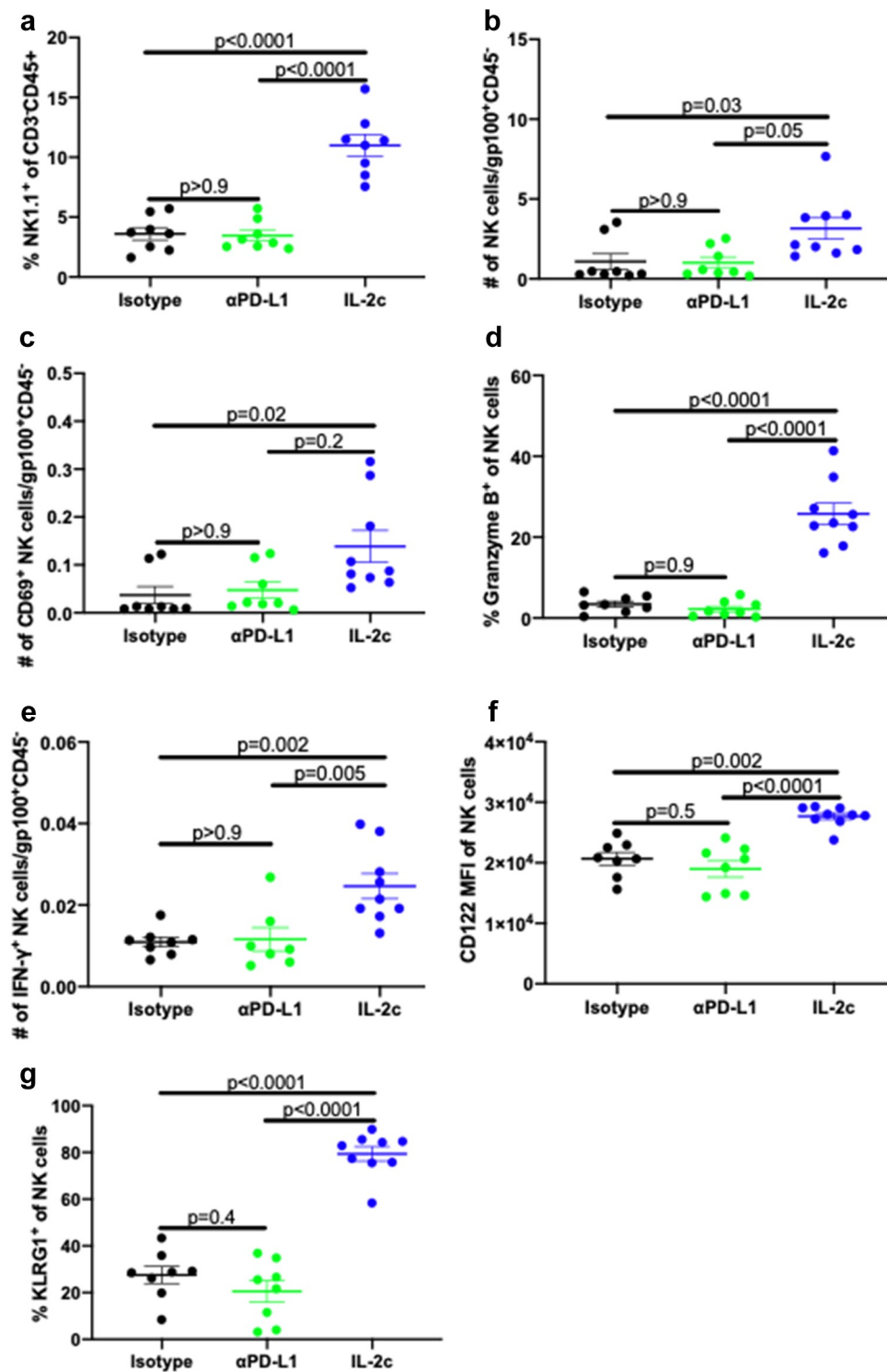


Figure 7. IL-2c promotes CD122 expression and NK cell maturation in B16 lung metastases. Wild-type male mice were challenged intravenously with 3×10^5 B16 cells and treated with 100 μ g α PD-L1 on days 14, 19, or IL-2c on days 14, 16, 18, or isotype control, and sacrificed on day 20. Total lung NK cell frequency (a) and tumor-normalized NK cell number (b), CD69 expression (c), granzyme B production (d), IFN- γ production (e), CD122 expression (f), and KLRG1 expression (g). $N = 5-9$ mice/group. p value, one-way ANOVA. ANOVA, analysis of variance. IFN- γ , interferon-gamma. IL-2c, interleukin-2 complex. KLRG1, Killer Cell Lectin Like Receptor G1. MFI, Mean Fluorescence Intensity. NK, Natural Killer. PD-L1, Programmed Death Ligand 1.

CD8⁺ T cells (or tumor-specific immunity), as we found that IL-2c efficacy was preserved in RAG^{KO} mice lacking any tumor-specific immunity. Flow cytometry analyses of B16 lung tumors showed that IL-2c preferentially boosts lung NK cell activation and effector function but not lung CD8⁺ T cells,

confirming the necessity of NK cells in IL-2c treatment of B16 lung metastasis and providing a striking contrast to peritoneal B16 tumors where IL-2c activated both CD8⁺ T and NK cells. We also identified an increase in lung KLRG1⁺ NK cells following IL-2c treatment, which denotes a terminally mature NK cell

population with a protective effect against pulmonary metastasis.^{46,47} The robust effects on this population in both bladder and lung following IL-2c treatment warrants further investigation, as IL-2c-driven NK cell maturation may occur via a CD122-Eomes axis,⁴⁸ with expansion of KLRG1⁺ NK cells serving as a possible biomarker for responsiveness to CD122-directed immunotherapies. In this regard, our NK cell immunophenotyping generally agrees with prior reports.²⁹ However, as tissue-specific NK cell differences are known,⁴⁹ detailed NK cell studies in specific anatomic compartments with tumor metastases will help further understanding of immunotherapy effects. Thus, detailed understandings of the immune landscape in distinct anatomic compartments and effects of specific treatment agents therein will help define more effective treatment regimens.

All together, we establish differential responsiveness of the same tumor to the same agent in distinct (metastatic) compartments, and IL-2c mechanisms of efficacy appear largely to depend on NK cells, whereas α PD-L1 effects depend to a greater extent on CD8⁺ T cells. These data suggest that combining α PD-L1 with IL-2c could be more effective against a variety of cancers, including in metastatic settings where there is a great unmet medical need. Further, other CD122-selective treatment approaches under evaluation, such as pegylated IL-2 (bempegaldesleukin) which shows efficacy in metastatic melanoma trials in combination with the α PD-1 agent, nivolumab,⁵⁰ should be similarly tested. It remains to be seen whether distinct CD122-targeted IL-2 constructs have differing capacities to activate CD8⁺ T cells versus NK cells or $\gamma\delta$ T cells, but such data will greatly help define optimal combinations for further clinical evaluations.

Abbreviations

Analysis of variance (ANOVA), asialo GM1 (asGM1), Bacillus Calmette-Guérin (BCG), bladder cancer (BC), cytotoxic T-lymphocyte-associate protein 4 (CTLA-4), Eomes (Eomesodermin), IL-2 complex (IL-2c), IL-2 receptor (IL-2R), immune checkpoint blockade (ICB), interleukin (IL), interferon-gamma (IFN- γ), killer cell lectin-like receptor G1 (KLRG1), mean fluorescence intensity (MFI), milligram (mg), natural killer (NK), programmed death receptor 1 (PD-1), programmed death-ligand 1 (PD-L1), recombination activating gene 1 (RAG1), T regulatory cells (Tregs), T cell receptor (TCR)

Acknowledgments

This work was supported by the Flow Cytometry Shared Resource Facility, which is supported by UL1 TR001120.

Disclosure statement

Ethics approval and consent to participate: All animal studies were approved by the UT Health San Antonio Institutional Animal Care and Use Committee and each experiment was conducted in accordance with the standards required by the UT Health San Antonio Department of Laboratory Animal Resources.

Funding

R. Reyes (NIH T32GM113896, NIH/NCATS TL1 TR002647, NIA T32 AG 021890), YD (CPRIT Research Training Award (RP 170345) and Ovarian Cancer Research Alliance Ann and Sol Schreiber Mentored Investigator Award), NM (CPRIT Research Training Award (RP170345)), RS (8KL2 TR000118, K23, P30 CA054174, Roger L. And Laura D. Zeller Charitable Foundation Chair in Urologic Cancer, CDMRP CA170270/P1P2), T. Curiel (CA054174, CA205965, CDMRP, The Owens Foundation, The Skinner endowment, The Barker endowment, P30 CA054174) and the National Center for Advancing Translational Sciences, National Institutes of Health, through Grant UL1 TR002645.

Consent for publication

All authors of this manuscript consent to its submission and publication.

Availability of data and material

The datasets used and/or analyzed during the current study are available from the corresponding author upon reasonable request.

Authors' contributions (CRediT – Contributor Roles Taxonomy)

RMR: conceptualization, data curation, formal analysis, funding acquisition, investigation, methodology, project administration, validation, visualization, writing – original draft, writing – review and editing. CZ: data curation, formal analysis, investigation, methodology, visualization, writing – original draft, and writing – review and editing. YD: data curation, formal analysis, investigation, methodology, visualization, and writing – review and editing. NJ: investigation, methodology, resources. NM: data curation, methodology, resources. ASP: investigation, resources. CAC: investigation. RSS: conceptualization, data curation, formal analysis, funding acquisition, resources, supervision, and writing – review and editing. TJC: conceptualization, data curation, formal analysis, funding acquisition, methodology, project administration, resources, software, supervision, writing – original draft, writing – review and editing.

References

1. Siegel RL, Miller KD, Jemal A. Cancer statistics, 2020. *CA Cancer J Clin.* 2020;70(1):7–15. doi:10.3322/caac.21590.
2. Suhail Y, Cain MP, Vanaja K, Kurywachak PA, Levchenko A, Kalluri R. Kshitiz: systems biology of cancer metastasis. *Cell Syst.* 2019;9(2):109–127. doi:10.1016/j.cels.2019.07.003.
3. Riggi N, Aguet M, Stamenkovic I. Cancer metastasis: a reappraisal of its underlying mechanisms and their relevance to treatment. *Annu Rev Pathol.* 2018;13(1):117–140. doi:10.1146/annurev-pathol-020117-044127.
4. Ganesh K, Massagué J. Targeting metastatic cancer. *Nat Med.* 2021;27(1):34–44. doi:10.1038/s41591-020-01195-4.
5. Chensue SW, Warmington KS, Ruth JH, Sanghi PS, Lincoln P, Kunkel SL. Role of monocyte chemoattractant protein-1 (MCP-1) in Th1 (mycobacterial) and Th2 (schistosomal) antigen-induced granuloma formation: relationship to local inflammation, Th cell expression, and IL-12 production. *J Immunol.* 1996;157:4602–4608.
6. Tas F. Metastatic behavior in melanoma: timing, pattern, survival, and influencing factors. *J Oncol.* 2012;2012:1–9. doi:10.1155/2012/647684.

7. Shinagare AB, Ramaiya NH, Jagannathan JP, Fennessy FM, Taplin M-E, Van Den Abbeele AD. Metastatic pattern of bladder cancer: correlation with the characteristics of the primary tumor. *Am J Roentgenol.* 2011;196(1):117–122. doi:10.2214/AJR.10.5036.
8. Flanagan M, Solon J, Chang KH, Deady S, Moran B, Cahill R, Shields C, Mulsow J. Peritoneal metastases from extra-abdominal cancer - A population-based study. *Eur J Surg Oncol.* 2018;44(11):1811–1817. doi:10.1016/j.ejso.2018.07.049.
9. Hegde PS, Chen DS. Top 10 challenges in cancer immunotherapy. *Immunity.* 2020;52(1):17–35. doi:10.1016/j.immuni.2019.12.011.
10. Gutzmer R, Stroyakovskiy D, Gogas H, Robert C, Lewis K, Protzenko S, Pereira RP, Eigentler T, Rutkowski P, Demidov L, *et al.* Atezolizumab, vemurafenib, and cobimetinib as first-line treatment for unresectable advanced BRAF(V600) mutation-positive melanoma (IMspire150): primary analysis of the randomised, double-blind, placebo-controlled, phase 3 trial. *Lancet (London, England).* 2020;395(10240):1835–1844. doi:10.1016/S0140-6736(20)30934-X.
11. Hamid O, Molinero L, Bolen CR, Sosman JA, Muñoz-Couselo E, Kluger HM, McDermott DF, Powderly JD, Sarkar I, Ballinger M, *et al.* Safety, clinical activity, and biological correlates of response in patients with metastatic melanoma: results from a phase I trial of atezolizumab. *Clin Cancer Res.* 2019;25(20):6061–6072. doi:10.1158/1078-0432.CCR-18-3488.
12. Tawbi HA, Forsyth PA, Algazi A, Hamid O, Hodi FS, Moschos SJ, Khushalani NI, Lewis K, Lao CD, Postow MA, *et al.* Combined nivolumab and Ipilimumab in melanoma metastatic to the brain. *N Engl J Med.* 2018;379(8):722–730. doi:10.1056/NEJMoa1805453.
13. Darvin P, Toor SM, Nair VS, Elkord E. Immune checkpoint inhibitors: recent progress and potential biomarkers. *Exp Mol Med.* 2018;50(12):1–11. doi:10.1038/s12276-018-0191-1.
14. Rosenberg SA, Lotze MT, Muul LM, Leitman S, Chang AE, Ettinghausen SE, Matory YL, Skibber JM, Shiloni E, Vetto JT, *et al.* Observations on the systemic administration of autologous lymphokine-activated killer cells and recombinant interleukin-2 to patients with metastatic cancer. *N Engl J Med.* 1985;313(23):1485–1492. doi:10.1056/NEJM198512053132327.
15. Krieg C, Létourneau S, Pantaleo G, Boyman O. Improved IL-2 immunotherapy by selective stimulation of IL-2 receptors on lymphocytes and endothelial cells. *Proc Natl Acad Sci U S A.* 2010;107(26):11906–11911. doi:10.1073/pnas.1002569107.
16. Arenas-Ramirez N, Woytschak J, Boyman O. Interleukin-2: biology, design and application. *Trends Immunol.* 2015;36(12):763–777. doi:10.1016/j.it.2015.10.003.
17. Malek TR. The biology of interleukin-2. *Annu Rev Immunol.* 2008;26(1):453–479. doi:10.1146/annurev.immunol.26.021607.090357.
18. Sakaguchi S, Sakaguchi N, Asano M, Itoh M, Toda M. Immunologic self-tolerance maintained by activated T cells expressing IL-2 receptor alpha-chains (CD25). Breakdown of a single mechanism of self-tolerance causes various autoimmune diseases. *J Immunol.* 1995;155:1151–1164.
19. Drerup JM, Deng Y, Pandeswara SL, Padrón AS, Reyes RM, Zhang X, Mendez J, Liu A, Clark CA, Chen W, *et al.* CD122-selective IL2 complexes reduce immunosuppression, promote treg fragility, and sensitize tumor response to PD-L1 blockade. *Cancer Res.* 2020;80(22):5063–5075. doi:10.1158/0008-5472.CAN-20-0002.
20. Reyes RM, Deng Y, Zhang D, Ji N, Mukherjee N, Wheeler K, Gupta HB, Padron AS, Kancharla A, Zhang C, *et al.* CD122-directed interleukin-2 treatment mechanisms in bladder cancer differ from aPD-L1 and include tissue-selective $\gamma\delta$ T cell activation. *J Immunother Cancer.* 2021;9(4):e002051. doi:10.1136/jitc-2020-002051.
21. Diab A, Tannir NM, Bentebibel S-E, Hwu P, Papadimitrakopoulou V, Haymaker C, Kluger HM, Gettinger SN, Sznol M, Tykodi SS. Bempagdesleukin (NKTR-214) plus nivolumab in patients with advanced solid tumors: phase I dose-escalation study of safety, efficacy, and immune activation (PIVOT-02). *Cancer Discov.* 2020;10(8):1158–1173. doi:10.1158/2159-8290.CD-19-1510.
22. Zhang D, Reyes RM, Osta E, Kari S, Gupta HB, Padron AS, Kornepati AV, Kancharla A, Sun X, Deng Y. Bladder cancer cell-intrinsic PD-L1 signals promote mTOR and autophagy activation that can be inhibited to improve cytotoxic chemotherapy. *Cancer Med.* 2021;10(6):2137–2152. doi:10.1002/cam4.3739.
23. Lyon A, Fallon J, Boyerinas B, Schmitz R, Hance KW, Lan Y, Sabzevari H, Tsang K, Schlom J, Greiner J. Anti-tumor effects of anti-PD-L1 therapy in an orthotopic bladder tumor model. *J Immunother Cancer.* 2014;2(S3):P101. doi:10.1186/2051-1426-2-S3-P101.
24. Clark CA, Gupta HB, Sareddy G, Pandeswara S, Lao S, Yuan B, Drerup JM, Padron A, Conejo-Garcia J, Murthy K. Tumor-intrinsic PD-L1 signals regulate cell growth, pathogenesis, and autophagy in ovarian cancer and melanoma. *Cancer Res.* 2016;76(23):6964–6974. doi:10.1158/0008-5472.CAN-16-0258.
25. Svatek RS, Zhao XR, Morales EE, Jha MK, Tseng TY, Hugen CM, Hurez V, Hernandez J, Curiel TJ. Sequential intravesical mitomycin plus bacillus calmette-guérin for non-muscle-invasive urothelial bladder carcinoma: translational and phase I clinical trial. *Clin Cancer Res.* 2015;21(2):303–311. doi:10.1158/1078-0432.CCR-14-1781.
26. Boyman O, Kovar M, Rubinstein MP, Surh CD, Sprent J. Selective stimulation of T cell subsets with antibody-cytokine immune complexes. *Science.* 2006;311(5769):1924–1927. doi:10.1126/science.1122927.
27. Tait Wojno ED, Beamer CA. Isolation and identification of innate lymphoid cells (ILCs) for immunotoxicity testing. *Methods Mol Biol.* 2018;1803:353–370.
28. Hayakawa Y, Smyth MJ. CD27 dissects mature NK cells into two subsets with distinct responsiveness and migratory capacity. *J Immunol.* 2006;176(3):1517–1524. doi:10.4049/jimmunol.176.3.1517.
29. Abel AM, Yang C, Thakar MS, Malarkannan S. Natural killer cells: development, maturation, and clinical utilization. *Front Immunol.* 2018;9:1869. doi:10.3389/fimmu.2018.01869.
30. Nishikado H, Mukai K, Kawano Y, Minegishi Y, Karasuyama H. NK cell-depleting anti-asialo GM1 antibody exhibits a lethal off-target effect on basophils in vivo. *J Immunol.* 2011;186(10):5766–5771. doi:10.4049/jimmunol.1100370.
31. Simonetta F, Pradier A, Roosnek E. T-bet and eomesodermin in NK cell development, maturation, and function. *Front Immunol.* 2016;7:241. doi:10.3389/fimmu.2016.00241.
32. Chiossone L, Chaix J, Fuseri N, Roth C, Vivier E, Walzer T. Maturation of mouse NK cells is a 4-stage developmental program. *Blood J Am Soc Hematol.* 2009;113:5488–5496.
33. Gasteiger G, Hemmers S, Firth MA, Le Floch A, Huse M, Sun JC, Rudensky AY. IL-2-dependent tuning of NK cell sensitivity for target cells is controlled by regulatory T cells. *J Exp Med.* 2013;210(6):1167–1178. doi:10.1084/jem.20122462.
34. Arenas-Ramirez N, Zou C, Popp S, Zingg D, Brannetti B, Wirth E, Calzascia T, Kovarik J, Sommer L, Zenke G. Improved cancer immunotherapy by a CD25-mimobody conferring selectivity to human interleukin-2. *Sci Transl Med.* 2016;8(367):367ra166–367ra166. doi:10.1126/scitranslmed.aag3187.
35. Oyer JL, Gitto SB, Altomare DA, Copik AJ. PD-L1 blockade enhances anti-tumor efficacy of NK cells. *Oncoimmunology.* 2018;7(11):e1509819. doi:10.1080/2162402X.2018.1509819.
36. Padrón Á, Hurez V, Gupta HB, Clark CA, Pandeswara SL, Yuan B, Svatek RS, Turk MJ, Drerup JM, Li R, *et al.* Age effects of distinct immune checkpoint blockade treatments in a mouse melanoma model. *Exp Gerontol.* 2018;105:146–154. doi:10.1016/j.exger.2017.12.025.
37. Ji S, Lee J, Lee ES, Kim DH, and Sin JI. B16 melanoma control by anti-PD-L1 requires CD8+ T cells and NK cells: application of anti-PD-L1 Abs and Trp2 peptide vaccines. *Hum Vaccin Immunother.* 2021;17(7): 1910–1922. PMID: 33522416
38. Gómez-Cuadrado L, Tracey N, Ma R, Qian B, Brunton VG. Mouse models of metastasis: progress and prospects. *Dis Model Mech.* 2017;10(9):1061–1074. doi:10.1242/dmm.030403.

39. Damsky WE, Rosenbaum LE, Bosenberg M. Decoding melanoma metastasis. *Cancers*. 2010;3(1):126–163. doi:10.3390/cancers3010126.
40. Babaian RJ, Johnson DE, Llamas L, Ayala AG. Metastases from transitional cell carcinoma of urinary bladder. *Urology*. 1980;16(2):142–144. doi:10.1016/0090-4295(80)90067-9.
41. Gelbart Y, Frankenburg S, Pinchasov Y, Krispel S, Eliahu D, Drize O, Morag E, Bartfeld D, Lotem M, Peretz T, *et al.* Production and purification of melanoma gp100 antigen and polyclonal antibodies. *Protein Expr Purif*. 2004;34(2):183–189. doi:10.1016/j.pep.2003.12.006.
42. Vaddepally RK, Kharel P, Pandey R, Garje R, Chandra AB. Review of indications of FDA-approved immune checkpoint inhibitors per NCCN guidelines with the level of evidence. *Cancers*. 2020;12(3):738. doi:10.3390/cancers12030738.
43. Sun J-Y, Zhang D, Wu S, Xu M, Zhou X, Lu X-J, Ji J. Resistance to PD-1/PD-L1 blockade cancer immunotherapy: mechanisms, predictive factors, and future perspectives. *Biomarker Res*. 2020;8(1):1–10. doi:10.1186/s40364-020-00212-5.
44. Ji N, Mukherjee N, Shu Z-J, Reyes RM, Meeks JJ, McConkey DJ, Gelfond JA, Curiel TJ, Svatek RS. $\gamma\delta$ T cells support antigen-specific $\alpha\beta$ T cell-mediated antitumor responses during BCG treatment for bladder cancer. *Cancer Immunol Res*. 2021. doi:10.1158/2326-6066.CIR-21-0285.
45. Ji N, Mukherjee N, Reyes RM, Gelfond J, Javors M, Meeks JJ, McConkey DJ, Shu Z-J, Ramamurthy C, Dennett R. Rapamycin enhances BCG-specific $\gamma\delta$ T cells during intravesical BCG therapy for non-muscle invasive bladder cancer: a randomized, double-blind study. *J ImmunoTher Cancer*. 2021;9(3):e001941. doi:10.1136/jitc-2020-001941.
46. Malaisé M, Rovira J, Renner P, Eggenhofer E, Sabet-Baktach M, Lantow M, Lang SA, Koehl GE, Farkas SA, Loss M, *et al.* KLRG1+ NK cells protect T-bet-deficient mice from pulmonary metastatic colorectal carcinoma. *J Immunol*. 2014;192(4):1954–1961. doi:10.4049/jimmunol.1300876.
47. Huntington ND, Tabarias H, Fairfax K, Brady J, Hayakawa Y, Degli-Esposti MA, Smyth MJ, Tarlinton DM, Nutt SL. NK cell maturation and peripheral homeostasis is associated with KLRG1 up-regulation. *J Immunol*. 2007;178(8):4764–4770. doi:10.4049/jimmunol.178.8.4764.
48. Zhang J, Marotel M, Fauteux-Daniel S, Mathieu AL, Viel S, Marçais A, Walzer T. T-bet and Eomes govern differentiation and function of mouse and human NK cells and ILC1. *Eur J Immunol*. 2018;48(5):738–750. doi:10.1002/eji.201747299.
49. Goh W, Huntington ND. Regulation of murine natural killer cell development. *Front Immunol*. 2017;8:130. doi:10.3389/fimmu.2017.00130.
50. Hurwitz M, Cho D, Balar A, Curti B, Siefker-Radtke A, Sznol M, Kluger H, Bernatchez C, Fanton C, Iacucci E, *et al.* Baseline tumor immune signatures associated with response to bempegaldesleukin (NKTR-214) and nivolumab. *J Clin Oncol*. 2019;37(15_suppl): Abstract 2623. doi:10.1200/JCO.2019.37.15_suppl.2623.